Pergamon

Materials Research Bulletin 37 (2002) 981–989

Materials Research Bulletin

Insertion of trivalent cations in the layered MPS_3 (Mn, Cd) materials

D. Ruiz-León[a], V. Manríquez[a,*], J. Kasaneva[b], R.E. Avila[c]

[a]*Departamento de Química, Facultad de Ciencias, Universidad de Chile, Casilla 653, Santiago, Chile*
[b]*Facultad de Ciencias Básicas, Universidad de Antofagasta, Antofagasta, Chile*
[c]*Departamento de Investigación y Desarrollo, Comisión Chilena de Energía Nuclear, Casilla 188-D, Santiago, Chile*

(Refereed)
Received 6 August 2001; accepted 7 January 2002

Abstract

The $Al_{0.21}Mn_{0.78}PS_3$, $Al_{0.15}Cd_{0.83}PS_3$, $In_{0.20}Cd_{0.70}PS_3$ and $Ga_{0.28}Cd_{0.58}PS_3$ compounds have been synthesized by the cation-exchange process used for other cationic species of the same family. These compounds were characterized by X-ray diffraction , Fourier transform infrared spectroscopy, ICP plasma analyses, photoconductivity and electrochemical impedance spectroscopy. The compounds synthesized show electrical conductivities (σ) of the order of 10^{-9} to 10^{-10} S cm^{-1} at 298 K and photoconductive effect. The physical properties of the new Al^{3+} materials reveal the same behavior as our previous report on In^{3+} and Ga^{3+} compounds.

Keywords: A. Chalcogenides; A. Layered compounds; D. Electrical properties

1. Introduction

The layered chalcogenides of transition metals, MPS_3, have attracted the attention of many workers, both by their anisotropic physical properties and potential technological applications [1,2].

The structure of these MPS_3 layered compounds is related to that of $CdCl_2$ with the transition metals and P–P pairs occupying the cadmium positions and sulphur atoms occupying the chloride positions [3]. This system is composed of stacking of

* Corresponding author. Tel.: +56-2-6787-251; fax: +56-2-2713-888.
E-mail address: vmanriqu@uchile.cl (V. Manríquez).

0025-5408/02/$ – see front matter
PII: S0025-5408(02)00719-5

sulphur-based sandwich layers weakly bonded by van der Waals forces. The MPS_3 phases form a class of lamellar materials structurally related to the well-known transition metal dichalcogenides. Similar chemical properties accompany this structural analogy. Thus, they can undergo a classical intercalation by electron donor species like alkali metals, amines or organometallic compounds. It has been shown that MPS_3 gives rise to an intercalation chemistry by a cation-transfer mechanism based on the ability of the material to insert cations, giving intercalations compounds in which the electrical charge is balanced by the loss of transition metal cations from the layers [4]. This cation-transfer intercalation route was extensively studied for the intercalation of monocations such as, K^+, $NH_4{}^+$ and cobaltocenium cations [5]. The multivalent cations Nd^{3+}, Sm^{3+} and Eu^{3+} have been inserted in $CdPS_3$ phases [6] and recently we have reported the insertion of In^{3+}, Ga^{3+} and $PANIH^+$ into $MnPS_3$ and $CdPS_3$ phases [7,8].

In order to explore the insertion of trivalent cations into the cadmium and manganese thiophosphates, and its effect on the physical properties, we report here the synthesis and characterization of the two new insertion compounds with aluminium, and its comparison with the In and Ga analogues.

2. Experimental

2.1. Preparation of host compounds

For the preparation of the host compounds, $MnPS_3$ and $CdPS_3$, the corresponding high purity powders (99.99%) were mixed in the stoichiometric amounts, sealed in evacuated quartz tubes, and heated at 1023 K for 2 weeks. After the reaction was completed, the reacted matter was cooled at room temperature. Homogeneous materials were obtained after grinding and reheating at 1023 K for 1 week.

2.2. Preparation of intercalated compounds

The intermediate intercalation compounds, $K_{2x}M_{1-x}PS_3$, were prepared according to the procedure previously described by Clément et al. [4]. The intercalation in $CdPS_3$ requires the presence of EDTA at pH $\sim$10 as complexing agent for the Cd^{2+} cations. The insertion of the trivalent cations was performed by treatment of the $K_{2x}M_{1-x}PS_3$ intermediate phase with an aqueous solution containing the cation (+3). In a typical experiment, 300 mg of the $K_{2x}M_{1-x}PS_3$ powder was stirred with 20 ml of a 0.3 mol l^{-1} aqueous solutions of the $AlCl_3$ salt for about 48 h at room temperature. The resulting products were repeatedly washed with water and dried at 10^{-3} Torr and 300 K.

2.3. Characterization

Both the host and intercalation compounds were characterized by various techniques. Powder X-ray diffraction (XRD) patterns were recorded in the range

$5^\circ < 2\theta < 60^\circ$ at room temperature, with a Siemens D-5000 diffractometer, using Cu Kα radiation. The IR spectra were obtained in the frecuency range 200–4000 cm^{-1} for samples pressed into KBr disks, with a Perkin Elmer

IR spectrophotometer system 2000. The elemental composition of the samples was obtained by ICP spectroscopy.

The electrical conductivity was measured by alternating current (ac) and direct current (dc) methods in the temperature range of 20–300°C. The two opposite flat surfaces of the samples were sputtered with gold and sandwiched between the platinum electrodes of the conductivity cell. Impedance measurements were carried out by a Solartron SI 1260 impedance gain-phase analyzer in the frequency range from 0.1 Hz to 10 MHz with a signal level between 50 mV and 1 V, to probe the charge transport mechanism. Direct current measurements were performed with a Keithley 237 source-meter, to ascertain the existence of slow relaxation mechanisms that may not be accessible through the impedance measurements.

Photoconductivity measurements were carried out in a cryostat at temperatures from 296 to 343 K, with vacuum of approximately 10^{-3} Torr. The samples, pressed into cylindrical disks of 13 mm diameter and 0.3 mm thickness, were mounted in a metallic holder, where illumination could be achieved through a transparent window. The light power density was 50 mW cm^{-2} from a Doolan Jenner Fiberlite A3200 halogen lamp. The current was recorded with a programmable Keithley 617 electrometer with silver paint contacts and planar configuration of the electrodes. The Ohmic nature of the contacts was checked; there was no evidence of any nonlinearity in the *I–V* characteristics.

3. Results and discussion

The preparation of the materials follows the two-step topotactic cation-transfer process. The first step consists of the intercalation of the K^+ ion in a cationic transfer process. The metal M^{2+} must be removed to maintain the electroneutrality of the host. In a second step the intercalated K^+ is removed from the interlamellar space by cationic exchange between the K^+ and the trivalent cation in aqueous solution.

The intercalation of K^+ in the host was carried following the procedure reported by Clément et al. [4] and was monitored by XRD and Fourier transform infrared (FTIR) spectroscopy. The analysis of the powder XRD diffractograms shows a displacement of the (0 0 1) line towards smaller values of 2θ (Fig. 1). The interplanar distance calculated is 9.3 Å. The IR spectrum shows the typical splitting of the asymmetric stretching band $\nu(PS_3)$ into two absorption bands, indicating the distortion of the octahedron formed by the $P_2S_6^{4-}$ unit (Fig. 2). The stoichiometries of the intermediates are $K_{0.28}Mn_{0.86}PS_3$ and $K_{0.54}Cd_{0.73}PS_3$. The insertion of trivalent cations is carried out by treating the precursor $K_{2x}M_{1-x}PS_3 \cdot H_2O$ with a salt solution of the trivalent cation. For the insertion of In^{3+} and Ga^{3+} the solution used was 1 M [7], however, for the insertion of aluminium a 0.3 M solution was used, due to the acidity of aluminium in solution, which causes a partial decomposition of the host phases.

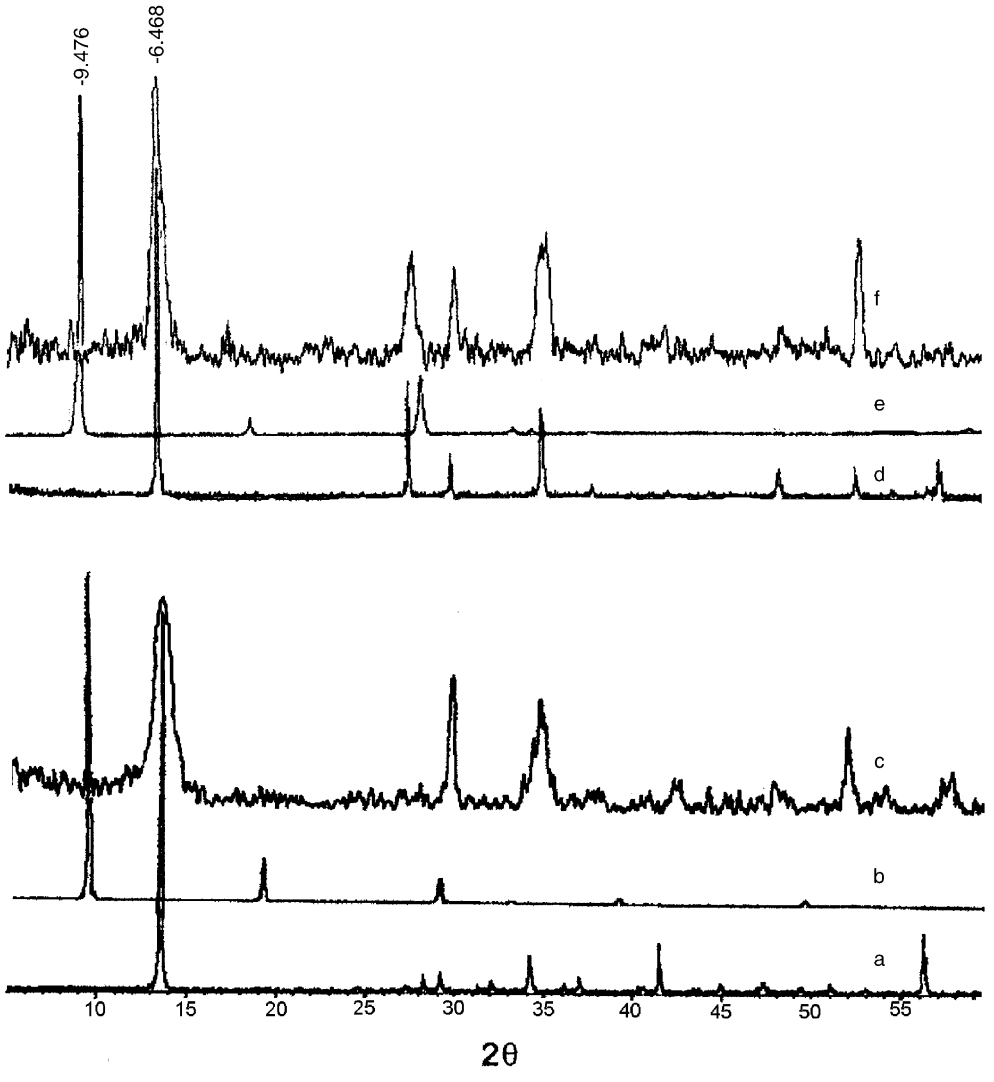

Fig. 1. XRD patterns of (a) $MnPS_3$, (b) $K_{0.28}Mn_{0.86}PS_3{\cdot}H_2O$, (c) $Al_{0.21}Mn_{0.78}PS_3$, (d) $CdPS_3$, (e) $K_{0.54}Cd_{0.73}S_3{\cdot}H_2O$, and (f) $Al_{0.15}Cd_{0.83}PS_3$.

The total incorporation of the ion (+3) is monitored by XRD and FTIR. The analysis of the XRD powder diffractograms shows that the interlaminar distances are close to those of the pristine phases and present some loss of crystallinity (Fig. 1). The IR spectrum shows that the $\nu(PS_3)$ band is not split (Fig. 2). Both XRD and IR spectra show that K^+ ion was removed from the layer. The elemental analysis shows the presence of the Al^{3+} and the absence of alkali metal in the final product. The calculated stoichiometries are $Al_{0.21}Mn_{0.78}PS_3$, $Al_{0.15}Cd_{0.83}PS_3$, $In_{0.20}Cd_{0.70}PS_3$ and $Ga_{0.28}Cd_{0.58}PS_3$. The analytical data for all of the insertion compounds obtained are summarised in Table 1.

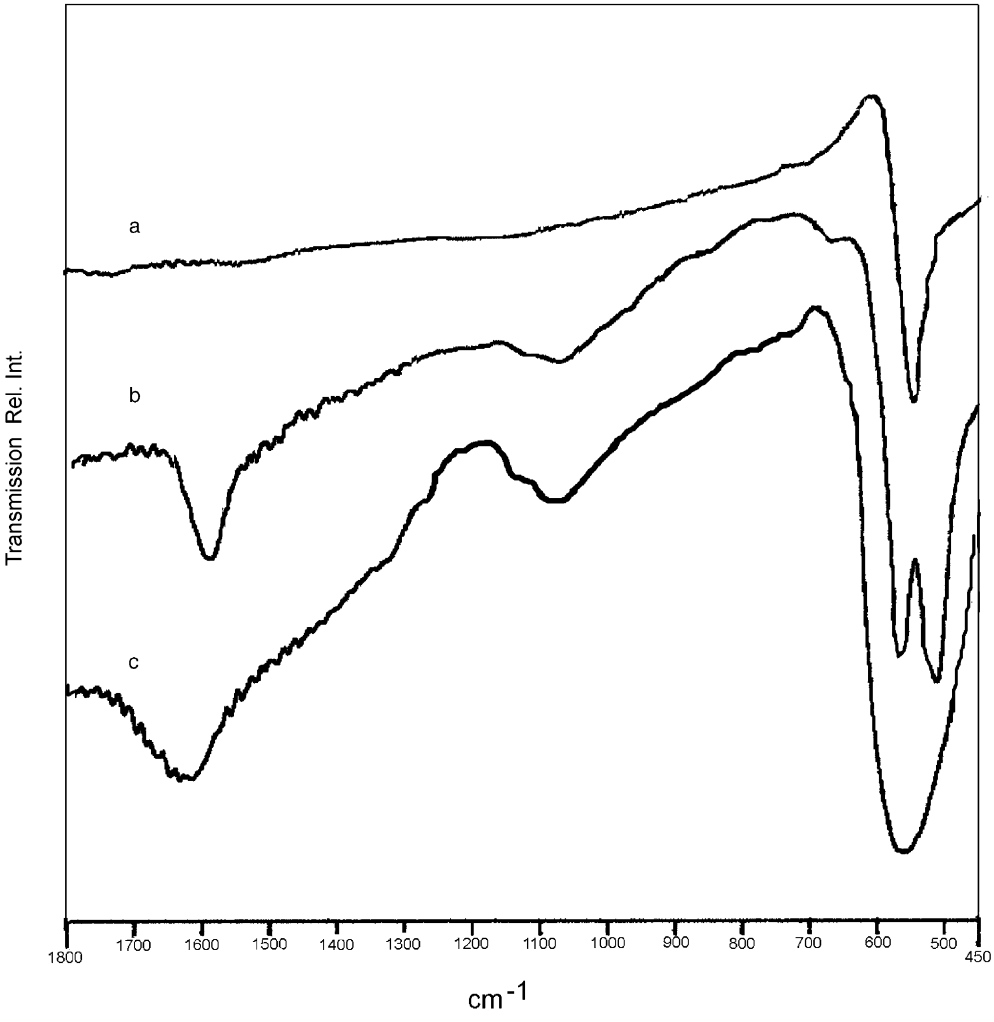

Fig. 2. FTIR spectra of (a) $CdPS_3$, (b) $K_{0.54}Cd_{0.73}S_3 \cdot H_2O$, and (c) $Al_{0.15}Cd_{0.83}PS_3$.

Table 1
Analytical data for the intercalates

Sample	Analytical data (wt.%)				
	Mn or Cd	P	S	K	Al, In or Ga
$K_{0.28}Mn_{0.86}PS_3$	23.20	15.20	47.30	5.38	–
$Al_{0.21}Mn_{0.78}PS_3$	21.10	15.90	46.70	–	2.58
$K_{0.54}Cd_{0.73}PS_3$	33.00	12.50	38.70	8.50	–
$Al_{0.15}Cd_{0.83}PS_3$	39.60	14.50	39.00	–	1.66
$In_{0.33}Cd_{0.50}PS_3$	24.60	13.56	42.11	–	16.59
$Ga_{0.28}Cd_{0.58}PS_3$	29.51	14.02	43.75	–	8.84

Table 2
Calculated values from dc method for conductivity (σ) at 298 K and values of light-induced defects (α) for pure and doped samples

Sample	σ (nS cm^{-1})	α
$MnPS_3$	300	0.0028
$Al_{0.21}Mn_{0.78}PS_3$	14.4	0.14
$CdPS_3$	190	0.05
$Al_{0.15}Cd_{0.83}PS_3$	27.6	0.20
$In_{0.33}Cd_{0.50}PS_3$	0.14	0.07
$Ga_{0.28}Cd_{0.58}PS_3$	1.40	0.04

The insertion of Al^{3+} cation into the $MnPS_3$ and $CdPS_3$ host matrix leads to a decrease in the conductivity values compared to the pristine starting materials. The same effect was evidenced with the insertion of other trivalent species, specifically indium and gallium trivalent cations. The σ values obtained from dc measurements are summarized in Table 2.

The impedance versus frequency measurements in the $Al_{0.21}Mn_{0.78}PS_3$ sample lead to Nyquist diagrams consisting of a single depressed arc, as shown in Fig. 3. The diagrams were obtained by letting the sample stabilize at 300°C, for 90 min, and then, measuring the cooling steps during which the overall scale (resistance and reactance) of the Nyquist arcs expanded by a factor of 2. The Nyquist arcs were fit to an equivalent circuit consisting of the parallel combination of a resistor (R_p) and a constant phase element (CPE), resulting in the values shown in Table 3. The CPE represents a distribution of relaxation times, leading to the admittance $Y = Q(i\omega)^n$, which corresponds to a single relaxation time, by an ideal capacitor, if $n = 1$.

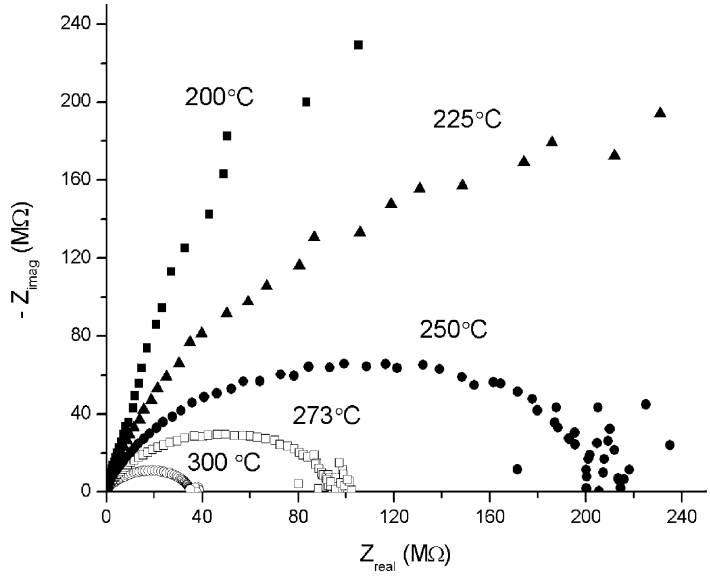

Fig. 3. Nyquist diagram from $Al_{0.21}Mn_{0.78}PS_3$ sample at different temperatures.

Table 3
Direct current conductivity and average capacitance (Q) for the $Al_{0.21}Mn_{0.78}PS_3$ sample at various temperatures

T (°C)	R_p (MΩ)	σ (nS cm^{-1})	Q (pF)	n
200	1960	0.211	0.670	0.844
225	639	0.646	0.385	0.703
250	223	1.85	0.468	0.682
273	99.8	4.14	0.609	0.684
300	38.4	10.80	0.713	0.655

The transport process leading to the impedance arcs should be related to either the grain interior or the grain boundaries. Electrode polarization effects can be ruled out, as those are associated with capacitances of over 10^5 pF. Then, the intergrain capacitance should be a few orders of magnitude below that value. The value of the average capacitance, Q (Table 3), is close to the geometrical capacitance of the pellet (0.21 pF). Thus, associating the process to the intragrain conduction, a value of 2.21 is obtained for the average dielectric permittivity of the bulk material. The fact that the capacitance spreading parameter, n, is essentially stable, suggests that the transport mechanism, including the carrier activation, is not perturbed by elemental segregation or chemical transformations in the temperature range below 300°C.

The Arrhenius plot (Fig. 4) of the $Al_{0.21}Mn_{0.78}PS_3$ intragrain conductivity indicates that the ac conduction is of semiconductor type. It fits to a straight line with preexponential factor of 1.23 S cm^{-1}, and activation energy of 0.915 eV, at a

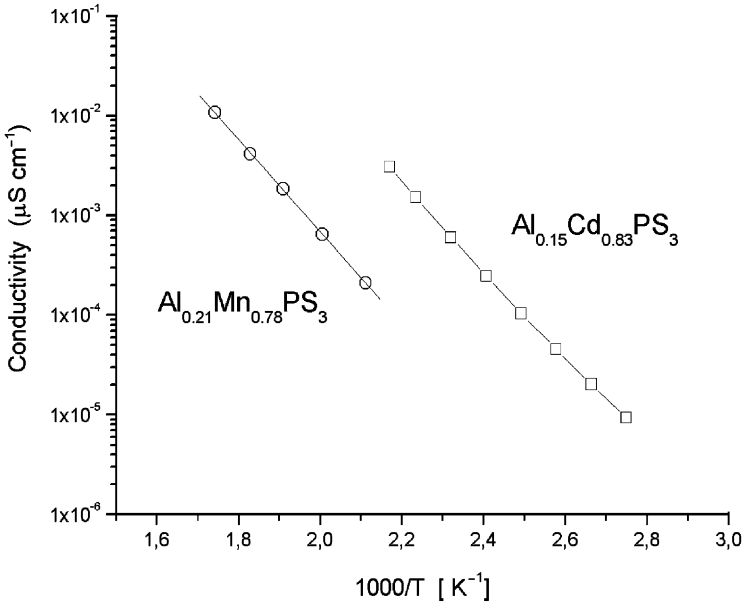

Fig. 4. Arrhenius plot for $Al_{0.21}Mn_{0.78}PS_3$ and $Al_{0.15}Cd_{0.83}PS_3$ samples.

correlation factor $r^2 = 0.9998$. Similarly, in the case of $Al_{0.15}Cd_{0.83}PS_3$, the Arrhenius plot (included in Fig. 4) fits an activation energy of 0.86 eV, preexponential factor of 5.6 S cm^{-1}, and $r^2 = 0.999$, after drying at 200°C.

The insertion compounds studied display photoconductive behaviour, although the current increase is small compared to the pristine phases. A peak in the rise curve is

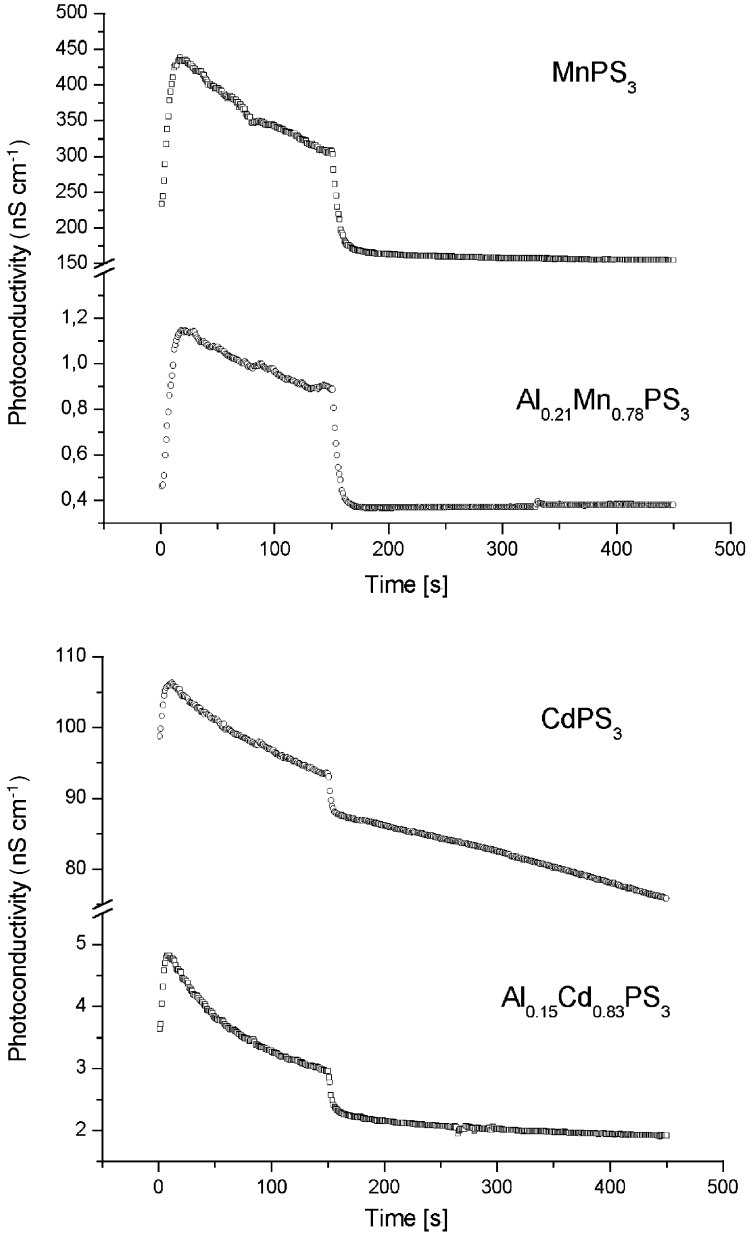

Fig. 5. Rise and decay of photoconductivity at 298 K for: $MnPS_3$, $Al_{0.21}Mn_{0.78}PS_3$, $CdPS_3$ and $Al_{0.15}Cd_{0.83}PS_3$.

observed in the present compounds. This peak has been attributed to the non-equilibrium recombination at higher intensities where the excess charge carrier density may be large. This type of anomalous behaviour in the rise curve has also been reported in other chalcogenides [9]. The $CdPS_3$ host phase and its inserted compound $Al_{0.15}Cd_{0.83}PS_3$ present a photoconductivity behaviour with a marked time dependence. Thus, the recorded conductivity shows a decrease with the illumination time. The values of σ at 150 s are smaller than the corresponding values at time 0 (Fig. 5). All the studied phases show persistent photoconductivity in the dark. These effects may be understood by assuming that deep traps are generated by the incident photons. Then, trapping of photogenerated carriers would build a space charge which would reduce the current during illumination. Their release, in the dark, would appear as the persistent photocurrent.

For explaining the effect in the host matrix of the trivalent inserted species (Al^{3+}, In^{3+} and Ga^{3+}) on the physical properties, we assumed that these species are in the intralamellar sites and generate free vacancies, these vacancies are responsible for the decrease in the conductivity values. In all of the cases the insertion of the trivalent species does not modify the general photoconductive tendency of the pristine material, but, as we can see in Table 2 in accordance with Hack et al. [10] the doped compounds present higher values in the rate of creation of defects by light or α parameter. This fact is in agreement with the observed decrease of the photoconductive effect. On the other hand, by using the simplified band structure described by Grasso et al. [11], the light exposure of the samples generating free holes in the P–S hybrid $3p_xp_y$ valence band orbital, the $3p_z$ valence band orbital can act as a recombination center.

Acknowledgments

Research financed by grants FONDECYT Nos. 2990014 and 1990972.

References

[1] A.H. Thompson, M.S. Whittingham, Mater. Res. Bull. 12 (1977) 741.
[2] R. Brec, Solid State Ionics 22 (1986) 3.
[3] W. Klingen, G. Eulenberger, H. Hahn, Z. Anorg. Allg. Chem. 401 (1973) 97.
[4] R. Clément, O. Garnier, J. Jegoudez, Inorg. Chem. 25 (1986) 1404.
[5] R. Clément, M. Doeuff, C. Gledel, J. Chim. Phys. 85 (1988) 1053.
[6] R. Clément, A. Leaustic, K. Marney, A.H. Francis, J. Phys. Chem. Solids 55 (1994) 9.
[7] V. Manríquez, A. Galdamez, A. Villanueva, P. Aranda, J.C. Galván, E. Ruiz-Hitzky, Mater. Res. Bull. 34 (1999) 673.
[8] V. Manríquez, A. Galdamez, J. Ponce, I. Brito, J. Kasaneva, Mater. Res. Bull. 34 (1999) 123.
[9] S.K. Tripathi, A. Kumar, J. Electron. Mater. 17 (1988) 45.
[10] M. Hack, S. Guha, W. den Boer, Phys. Rev. B 33 (1986) 2512.
[11] V. Grasso, F. Neri, S. Santangelo, L. Silipigni, M. Piacentini, Phys. Rev. B 37 (1988) 4419.